Unraveling the Nature of Sites Active toward Hydrogen Peroxide Reduction in Fe-N-C Catalysts

Chang Hyuck Choi,* Won Seok Choi, Olga Kasian, Anna K. Mechler, Moulay Tahar Sougrati, Sebastian Brüller, Kara Strickland, Qingying Jia, Sanjeev Mukerjee, Karl J. J. Mayrhofer, and Frédéric Jaouen*

Abstract: *Fe-N-C catalysts with high O_2 reduction performance are crucial for displacing Pt in low-temperature fuel cells. However, insufficient understanding of which reaction steps are catalyzed by what sites limits their progress. The nature of sites were investigated that are active toward H_2O_2 reduction, a key intermediate during indirect O_2 reduction and a source of deactivation in fuel cells. Catalysts comprising different relative contents of FeN_xC_y moieties and Fe particles encapsulated in N-doped carbon layers (0–100 %) show that both types of sites are active, although moderately, toward H_2O_2 reduction. In contrast, N-doped carbons free of Fe and Fe particles exposed to the electrolyte are inactive. When catalyzing the ORR, FeN_xC_y moieties are more selective than Fe particles encapsulated in N-doped carbon. These novel insights offer rational approaches for more selective and therefore more durable Fe-N-C catalysts.*

The oxygen reduction reaction (ORR), a key reaction for acidic fuel cells, is today most efficiently catalyzed by Pt materials.[1] However, the large-scale deployment of acidic fuel cells will be confronted with the grand challenge of developing inexpensive catalysts with high activity and stability.[2] While metal–nitrogen–carbon catalysts (M-N-C, especially M = Fe or Co) are promising,[3] further advances and fundamental insights into the factors governing their catalysis and durability are needed to meet the stringent industrial requirements.

The nature of active sites in pyrolyzed Fe-N-C catalysts is a highly complex and debated topic.[4] The simultaneous presence of multiple Fe species in most catalysts investigated hitherto has obscured the interpretation of their ORR behaviors, especially since multiple sites may lead to unexpected synergies. In particular, several types of active sites may be necessary to catalyze the multielectronic ORR, which may proceed either through a direct $4e^-$ pathway on a single site ($O_2 \rightarrow H_2O$), or through indirect pathways involving a desorbed H_2O_2 intermediate ($O_2 \rightarrow H_2O_2 \rightarrow H_2O$) on two sites. These may be identical in nature (consequential $2e^- \times 2e^-$ mechanism), or different (bifunctional $2e^- + 2e^-$ mechanism). If the ORR proceeds via the bifunctional mechanism, one type of site (S1) reduces O_2 to H_2O_2 and another (S2) catalyzes the peroxide reduction reaction (PRR). Under this hypothesis, only Fe-N-C catalysts comprising a high density of sites S1 and S2 may catalyze the ORR with an apparent low % H_2O_2. PRR catalysis is also highly desirable for improved durability of Fe-N-C catalysts because even low H_2O_2 production can lead to significant degradation during fuel cell operation.[5]

From advanced spectroscopy (Mössbauer[6] and X-ray absorption spectroscopy (XAS),[7] and mass spectrometry[8]) or molecular-probe approaches,[9] there is a growing consensus that FeN_xC_y moieties or N-C species encapsulating Fe particles (Fe@*N*-C) catalyze the transfer of the first $2e^-$ during ORR (S1).[10] Then, if the ORR mostly follows the $2e^- + 2e^-$ pathway, highly selective Fe-N-C catalysts should be characterized by a high number of sites S2.[11] It has been recently suggested that Fe particles or pyridinic-N groups might be the site S2.[12] However, improved understanding on

[*] Prof. C. H. Choi
School of Materials Science and Engineering, Gwangju Institute of Science and Technology
Gwangju 61005 (Republic of Korea)
E-mail: chchoi@gist.ac.kr

Dr. A. K. Mechler, Dr. M. T. Sougrati, Dr. S. Brüller, Dr. F. Jaouen
Université de Montpellier, Institut Charles Gerhardt Montpellier
2 place Eugène Bataillon, 34095 Montpellier (France)
E-mail: frederic.jaouen@umontpellier.fr

Dr. A. K. Mechler
Max Planck Institute for Chemical Energy Conversion
Stiftstraße 34–36, 45470 Mülheim a.d. Ruhr (Germany)

W. S. Choi, Dr. O. Kasian, Dr. K. Strickland, Prof. K. J. J. Mayrhofer
Max-Planck-Institut für Eisenforschung GmbH
Max-Planck-Strasse 1, 40237 Düsseldorf (Germany)

Prof. K. J. J. Mayrhofer
Helmholtz-Institute Erlangen-Nürnberg for
Renewable Energy Forschungszentrum
Jülich (Germany)

and

Department of Chemical and Biological Engineering
Friedrich-Alexander-Universität Erlangen-Nürnberg
Egerlandstrasse 3, 91058 Erlangen (Germany)

Dr. K. Strickland, Dr. Q. Jia, Prof. S. Mukerjee
Department of Chemistry and Chemical Biology
Northeastern University, Boston, MA 02115 (USA)

📄 Supporting information and the ORCID identification number(s) for
ⓘD the author(s) of this article can be found under:
https://doi.org/10.1002/anie.201704356.

the nature of the sites active toward PRR is still pivotal for improved durability. To determine whether Fe-N-C materials catalyze the ORR via a direct, consequential, or bifunctional mechanism, we have investigated the PRR activity on a set of catalysts, including model catalysts only comprising either FeN_xC_y moieties or Fe particles.

In the continuation of our recent studies,[10b,13] the catalysts were synthesized by pyrolysis of Fe^{II} acetate, 1,10-phenanthroline (Phen), and a Zn^{II} zeolitic imidazolate framework (ZIF-8). Three catalysts were first prepared, named FeNC-wet-1, FeNC-dry-1, and FeNC-dry-0.5, the labeling referring to homogenization conditions and Fe content before pyrolysis (see Methods in the Supporting Information). A catalyst pyrolyzed without Fe^{II} acetate was also prepared ("NC"). FeNC-wet-1, FeNC-dry-1, and FeNC-dry-0.5 showed Fe content of ca. 3.4, 3.0, and 1.5 wt% after pyrolysis, respectively, while about 100 ppm Fe was detected with inductively coupled plasma mass spectrometry (ICP-MS) for NC.[14] X-ray diffraction (XRD) and Raman spectroscopy revealed carbonization of ZIF-8 and Phen after pyrolysis (Supporting Information, Figure S1). X-ray photoelectron spectroscopy (XPS) shows similar N-doping level and *N*-components for all catalysts (Supporting Information, Figure S2, Table S1).
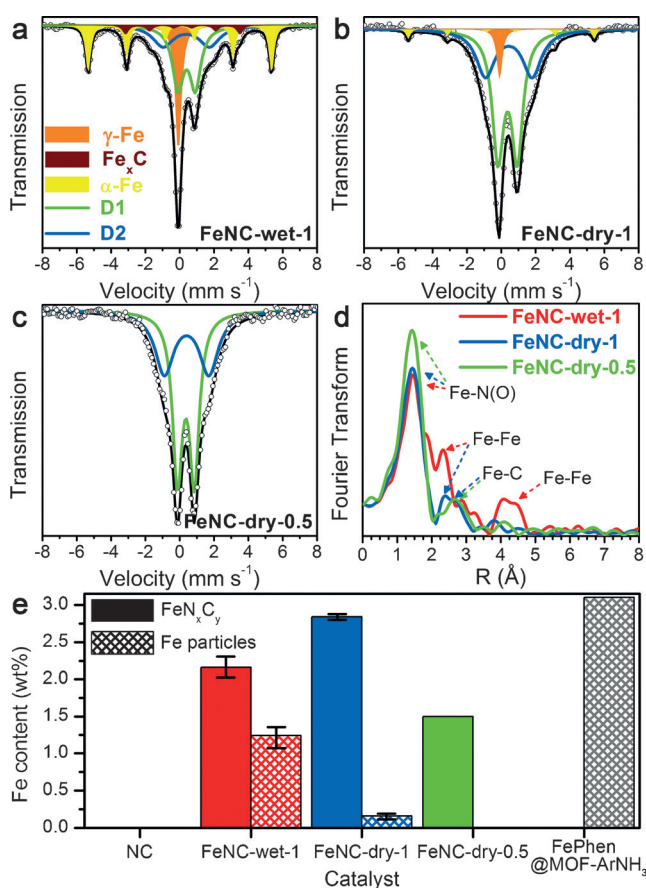
To identify the Fe structures in the catalysts, we examined their morphology with transmission electron microscopy (TEM), which revealed a larger number of Fe particles in FeNC-wet-1 than in FeNC-dry-1, with most Fe particles embedded in N-doped carbon layers (Supporting Information, Figure S3). ^{57}Fe Mössbauer spectroscopy showed that the crystalline Fe particles seen in TEM images correspond to α-Fe, Fe carbide, or γ-Fe (Figure 1 a–c; Supporting Information, Table S2). The relative absorption area owing to Fe particles was 47% for FeNC-wet-1 and 8% for FeNC-dry-1. No signal assigned to Fe particles was detected for FeNC-dry-0.5, the Mössbauer spectrum of which shows only the doublets D1 and D2 (FeN_xC_y moieties). These observations were confirmed by extended X-ray absorption fine structure (EXAFS), with a lower intensity of the Fe-Fe backscattering signal for FeNC-dry-1 vs. FeNC-wet-1 (Figure 1 d). As previously reported,[10b] a strong Fe-N(O) interaction without Fe-Fe interaction for FeNC-dry-0.5 confirms the sole presence of FeN_xC_y moieties. Quantification of the absolute content of each Fe component was derived from the Mössbauer spectra fittings (Figure 1 e).[6c] Thus, Fe-N-C catalysts with high (FeNC-wet-1) and low content (FeNC-dry-1) of Fe particles are identified, along with those devoid of Fe particles (FeNC-dry-0.5) and nearly devoid of Fe altogether (NC). Furthermore, a catalyst labeled FePhen@-MOF-ArNH$_3$ exclusively comprising Fe particles was investigated.[10a] Its Fe content was 3.1 wt% (Figure 1 e), with Fe being present as metallic, carbide, and nitride particles.

The electrochemical properties were then measured using a rotating disk electrode (RDE) in 0.1M $HClO_4$ electrolyte.
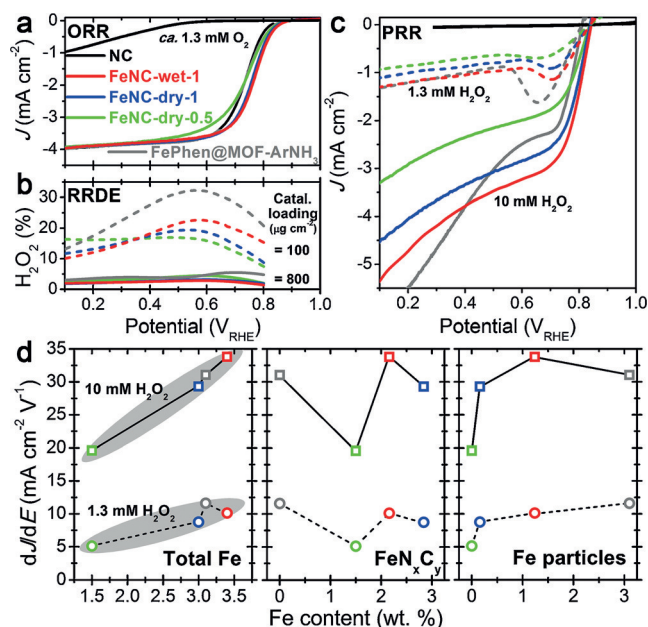

Figure 1. ^{57}Fe Mössbauer absorption spectra and their fittings with five spectral components for a) FeNC-wet-1, b) FeNC-dry-1, and c) FeNC-dry-0.5. d) Fourier transforms of the EXAFS spectra. e) Absolute Fe contents of the two main sub-groups of Fe species.

Figure 2. Electrochemical characterization. a) ORR polarization curves, b) H_2O_2 formation measured with RRDE, and c) PRR polarization curves: 900 rpm and 800 µg cm^{-2} (additionally, 100 µg cm^{-2} for RRDE studies). d) Correlations between PRR activity and absolute content of either total Fe or Fe sub-components. PRR activity is reported as the slope dJ/dE seen in (c) at high potential (see the Supporting Information).

All four of the Fe-N-C catalysts showed high ORR activity (Figure 2a), comparable to that of other high-performing Fe-N-C catalysts.[3c] The NC catalyst showed poor ORR kinetics, as expected in acidic medium.[4,10a,b] Rotating ring disk electrode (RRDE) measurements at $800\,\mu g\,cm^{-2}$ loading showed low H_2O_2 production ($<6\%$) during ORR for the four Fe-N-C catalysts (Figure 2b and S4). However, at $100\,\mu g\,cm^{-2}$, up to 32% H_2O_2 production was measured. This indicates that H_2O_2 produced at a given catalytic site may be consecutively reduced to H_2O. This suggests that, on some Fe sites at least, H_2O_2 may desorb and then re-adsorb on the same type or on another type of Fe sites having a higher affinity for H_2O_2. Furthermore, the positive correlation between % H_2O_2 and absolute content of Fe particles at low loading (Supporting Information, Figure S4, right) suggests FeN_xC_y moieties catalyze the ORR to H_2O more selectively than Fe@NC sites. Owing to 15–30% H_2O_2 produced during ORR at low loading, investigating the PRR activity of different sites in Fe-N-C catalysts is important to rationally improve their selectivity.

The PRR activity was measured in Ar-saturated $0.1\,M$ $HClO_4$ electrolyte containing 1.3 or 10 mM H_2O_2 (Figure 2c). The NC catalyst showed no PRR activity, indicating that surface N-groups unpromoted by Fe cannot be a site S2. In contrast, high PRR current on FeNC-dry-0.5 demonstrates that FeN_xC_y moieties are PRR-active. This is a first major finding of the present study, enabled by the synthesis of Fe-N-C catalysts free of Fe particles.[10b,15]

Previous work hypothesized that Fe-N-C catalysts catalyze the ORR via a bifunctional $2e^- + 2e^-$ mechanism in acidic medium; the site S1 for $2e^-$ ORR being FeN_xC_y moieties and site S2 for PRR being Fe particles.[12a] However, the turnover frequency of FeN_xC_y moieties for PRR is much lower than that for ORR (FeNC-dry-0.5: lower PRR than ORR current at $0.8\,V_{RHE}$ for the same reactant concentration of 1.3 mM, Figure 2a,c). This suggests that ORR on FeN_xC_y moieties predominantly occurs via the direct $4e^-$ pathway. This is also supported by the low H_2O_2 production measured for FeNC-dry-0.5 at low loading (Figure 2b).

At this stage, we however do not know yet whether Fe particles present in other Fe-N-C catalysts are PRR active. If such particles are PRR inactive, the PRR activity should be linearly correlated with the absolute FeN_xC_y content. However, no linear correlation between FeN_xC_y content and PRR activity is observed (Figure 2d, center). This suggests that FeN_xC_y sites are not the sole active site for PRR but that Fe particles should also be considered. Some correlation is observed between PRR activity and content of Fe particles (Figure 2d, right), but a better correlation is observed between PRR activity and the total Fe content (Figure 2d, left). Significant PRR activity of FePhen@MOF-ArNH$_3$ also demonstrates that Fe particles are PRR active, with an activity commensurate to those of FeN_xC_y moieties (Figure 2c,d).

While Fe particles are PRR-active, it is still unclear whether they need to be directly exposed to the electrolyte for catalyzing the PRR. Fe particles in direct contact with electrolyte have previously been suggested to be a site S2.[12a,16] Recently, we showed that electrolyte-exposed Fe
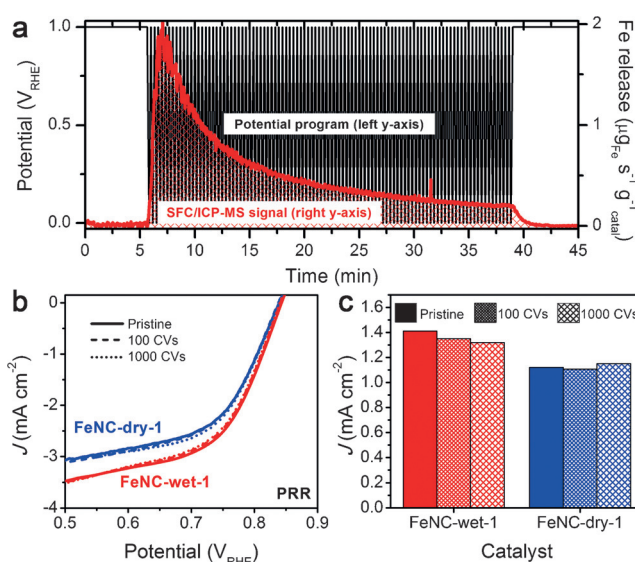

Figure 3. PRR activity before and after electrochemical dissolution of electrolyte-exposed Fe particles a) Fe dissolution rates from FeNC-wet-1 during 100 cycles. b) PRR polarization curves before and after 100 or 1000 cycles and c) PRR current density at $0.8\,V_{RHE}$ before and after the cycling.

particles can survive in acidic environments at $>0.7\,V_{RHE}$, which is due to stabilization of ferric hydroxide species.[13] The presence of Fe particles exposed to acidic electrolyte during short RDE studies is thus possible.

To elucidate whether Fe particles must be directly exposed to the electrolyte to catalyze the PRR, The PRR activity of FeNC-wet-1 and FeNC-dry-1 was measured before and after dissolution (electrochemical dissolution[13b]) of electrolyte-exposed particles (Figure 3). Operando analysis using a scanning flow cell (SFC) connected with ICP-MS (Supporting Information, Figure S5) showed that a significant fraction of electrolyte-exposed Fe particles in FeNC-wet-1 were removed during 100 cyclic voltammograms (CV) between 0 and 1 V_{RHE} (Figure 3a). The dissolved Fe reaches 9% of the total content of Fe particles present in pristine FeNC-wet-1. FeN_xC_y moieties are highly stable during this treatment, as previously demonstrated by negligible Fe leaching from FeNC-dry-0.5.[13b]

The PRR activity of FeNC-dry-1 and FeNC-wet-1 were however unmodified, even after extended dissolution up to 1000 CVs (Figure 3b and c). An extrapolation predicts that the vast majority of electrolyte-exposed Fe particles are removed after 1000 CVs (Supporting Information, Figure S6). As previously reported,[13] the dissolution of exposed Fe particles did not decrease the ORR activity (Supporting Information, Figure S7). Therefore, it is concluded that electrolyte-exposed Fe particles in pristine FeNC-wet-1 are inactive toward PRR and ORR. It demonstrates that Fe@N-C sites are therefore PRR active and can be a site S2, as previously hypothesized.[10a]

In conclusion, we elucidated the PRR and ORR reactivity of four different structures existing in Fe-N-C catalysts, that is, metal-free N-C groups, electrolyte-exposed Fe particles, FeN_xC_y moieties and Fe@N-C. The ORR pathways on Fe-
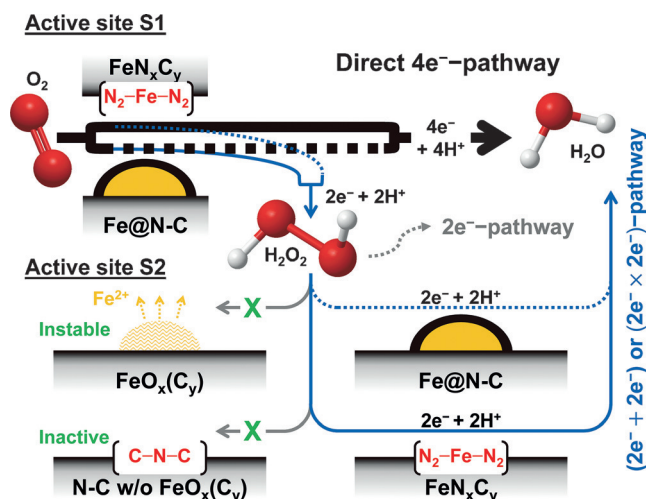
Figure 4. ORR mechanisms on Fe-N-C catalysts in acid medium. The site S1 is FeN_xC_y moieties or Fe@N-C. FeN_xC_y mostly catalyzes direct $4e^-$ ORR, but also releases a minor fraction of H_2O_2. Fe@N-C produces higher fraction of H_2O_2 in comparison to FeN_xC_y. The released H_2O_2 is then reduced to H_2O on site S2 (either FeN_xC_y or Fe@N-C). Surface-exposed Fe particles and N-groups without subsurface Fe are PRR-inactive.

N-C catalysts could consequently be established (Figure 4). Contrary to previous hypotheses, N-C groups and electrolyte-exposed Fe particles were shown to be inactive toward PRR in acidic medium. We also demonstrated that FeN_xC_y moieties and Fe@N-C species are moderately active toward PRR, proving their possible roles in both direct (major path) and indirect $4e^-$ ORR pathways. Since the synthesis of Fe-N-C catalysts with only FeN_xC_y moieties,[10b,15] only Fe@N-C particles,[10a] or their combination[3b,d,17] is now controllable, the understanding of the nature of active sites for PRR provided herein offers new insights for the rational design of advanced Fe-N-C catalysts with high selectivity and expectedly improved durability in polymer electrolyte fuel cells.

Acknowledgements

Conflict of interest

The authors declare no conflict of interest.

[1] C. H. Cui, L. Gan, M. Heggen, S. Rudi, P. Strasser, *Nat. Mater.* **2013**, *12*, 765.

[2] J. Shui, M. Wang, F. Du, L. Dai, *Sci. Adv.* **2015**, *1*, e1400129.

[3] a) R. Bashyam, P. Zelenay, *Nature* **2006**, *443*, 63; b) M. Lefèvre, E. Proietti, F. Jaouen, J. P. Dodelet, *Science* **2009**, *324*, 71; c) F. Jaouen, et al., *ACS Appl. Mater. Inter.* **2009**, *1*, 1623; d) G. Wu, K. L. More, C. M. Johnston, P. Zelenay, *Science* **2011**, *332*, 443; e) J. Y. Cheon, et al., *Sci. Rep.* **2013**, *3*, 2715; f) B. Y. Guan, L. Yu, X. W. Lou, *Energy Environ. Sci.* **2016**, *9*, 3092; g) B. Y. Xia, Y. Yan, N. Li, H. B. Wu, X. W. Lou, X. Wang, *Nat. Energy* **2016**, *1*, 15006; h) T. Liu, P. Zhao, X. Hua, W. Luo, S. Chen, G. Cheng, *J. Mater. Chem. A* **2016**, *4*, 11357.

[4] J. Masa, W. Xia, M. Muhler, W. Schuhmann, *Angew. Chem. Int. Ed.* **2015**, *54*, 10102; *Angew. Chem.* **2015**, *127*, 10240.

[5] V. Goellner, V. Armel, A. Zitolo, E. Fonda, F. Jaouen, *J. Electrochem. Soc.* **2015**, *162*, H403.

[6] a) J. Tian, A. Morozan, M. T. Sougrati, M. Lefèvre, R. Chenitz, J. P. Dodelet, D. Jones, F. Jaouen, *Angew. Chem. Int. Ed.* **2013**, *52*, 6867; *Angew. Chem.* **2013**, *125*, 7005; b) U. I. Kramm, M. Lefevre, N. Larouche, D. Schmeisser, J. P. Dodelet, *J. Am. Chem. Soc.* **2014**, *136*, 978; c) M. T. Sougrati, V. Goellner, A. K. Schuppert, L. Stievano, F. Jaouen, *Catal. Today* **2016**, *262*, 110.

[7] a) N. Ramaswamy, U. Tylus, Q. Y. Jia, S. Mukerjee, *J. Am. Chem. Soc.* **2013**, *135*, 15443; b) Q. Jia, et al., *ACS Nano* **2015**, *9*, 12496; c) J. Li, et al., *Energy Environ. Sci.* **2016**, *9*, 2418.

[8] a) M. Lefèvre, J. P. Dodelet, P. Bertrand, *J. Phys. Chem. B* **2005**, *109*, 16718; b) W. M. Li, J. Wu, D. C. Higgins, J. Y. Choi, Z. W. Chen, *ACS Catal.* **2012**, *2*, 2761.

[9] N. R. Sahraie, U. I. Kramm, J. Steinberg, Y. J. Zhang, A. Thomas, T. Reier, J. P. Paraknowitsch, P. Strasser, *Nat. Commun.* **2015**, *6*, 8618.

[10] a) K. Strickland, M. W. Elise, Q. Y. Jia, U. Tylus, N. Ramaswamy, W. T. Liang, M. T. Sougrati, F. Jaouen, S. Mukerjee, *Nat. Commun.* **2015**, *6*, 7343; b) A. Zitolo, V. Goellner, V. Armel, M.-T. Sougrati, T. Mineva, L. Stievano, E. Fonda, F. Jaouen, *Nat. Mater.* **2015**, *14*, 937; c) J. A. Varnell, E. C. M. Tse, C. E. Schulz, T. T. Fister, R. T. Haasch, J. Timoshenko, A. I. Frenkel, A. A. Gewirth, *Nat. Commun.* **2016**, *7*, 12582.

[11] a) T. S. Olson, S. Pylypenko, J. E. Fulghum, P. Atanassov, *J. Electrochem. Soc.* **2010**, *157*, B54; b) M. H. Robson, A. Serov, K. Artyushkova, P. Atanassov, *Electrochim. Acta* **2013**, *90*, 656; c) A. Serov, U. Tylus, K. Artyushkova, S. Mukerjee, P. Atanassov, *Appl. Catal. B* **2014**, *150*, 179.

[12] a) U. Tylus, Q. Jia, K. Strickland, N. Ramaswamy, A. Serov, P. Atanassov, S. Mukerjee, *J. Phys. Chem. C* **2014**, *118*, 8999; b) K. Artyushkova, A. Serov, S. Rojas-Carbonell, P. Atanassov, *J. Phys. Chem. C* **2015**, *119*, 25917.

[13] a) C. H. Choi, C. Baldizzone, J. P. Grote, A. K. Schuppert, F. Jaouen, K. J. J. Mayrhofer, *Angew. Chem. Int. Ed.* **2015**, *54*, 12753; *Angew. Chem.* **2015**, *127*, 12944; b) C. H. Choi, et al., *ACS Catal.* **2016**, *6*, 3136.

[14] G. Zhang, R. Chenitz, M. Lefèvre, S. Sun, J.-P. Dodelet, *Nano Energy* **2016**, *29*, 111.

[15] U. I. Kramm, I. Herrmann-Geppert, J. Behrends, K. Lips, S. Fiechter, P. Bogdanoff, *J. Am. Chem. Soc.* **2016**, *138*, 635.

[16] J. D. Wiggins-Camacho, K. J. Stevenson, *J. Phys. Chem. C* **2011**, *115*, 20002.

[17] E. Proietti, F. Jaouen, M. Lefevre, N. Larouche, J. Tian, J. Herranz, J. P. Dodelet, *Nat. Commun.* **2011**, *2*, 416.